SANDIA REPORT
SAND87—0889 • UC—34D
Unlimited Release
Printed September 1987

An Excitation-Term Modification for a Certain Class of Electromagnetic Aperture-Coupling Problems

Douglas J. Riley, Larry D. Bacon

Prepared by
Sandia National Laboratories
Albuquerque, New Mexico 87185 and Livermore, California 94550
for the United States Department of Energy
under Contract DE-AC04-76DP00789

When printing a copy of any digitized SAND Report, you are required to update the markings to current standards.

SF2900Q(8-81)

Issued by Sandia National Laboratories, operated for the United States Department of Energy by Sandia Corporation.

NOTICE: This report was prepared as an account of work sponsored by an agency of the United States Government. Neither the United States Government nor any agency thereof, nor any of their employees, nor any of their contractors, subcontractors, or their employees, makes any warranty, express or implied, or assumes any legal liability or responsibility for the accuracy, completeness, or usefulness of any information, apparatus, product, or process disclosed, or represents that its use would not infringe privately owned rights. Reference herein to any specific commercial product, process, or service by trade name, trademark, manufacturer, or otherwise, does not necessarily constitute or imply its endorsement, recommendation, or favoring by the United States Government, any agency thereof or any of their contractors or subcontractors. The views and opinions expressed herein do not necessarily state or reflect those of the United States Government, any agency thereof or any of their contractors or subcontractors.

Printed in the United States of America
Available from
National Technical Information Service
U.S. Department of Commerce
5285 Port Royal Road
Springfield, VA 22161

NTIS price codes
Printed copy: A03
Microfiche copy: A01

SAND87-0889
Unlimited Release
Printed September 1987

Distribution
Category UC-34D

An Excitation-Term Modification For a Certain Class of Electromagnetic Aperture-Coupling Problems

Douglas J. Riley
Electromagnetic Applications Division

Larry D. Bacon
Microwave Physics Division

Sandia National Laboratories
Albuquerque, New Mexico 87185

ABSTRACT

A simple technique is presented for modifying electromagnetic aperture-coupling integral equations that are based on an infinite-ground-plane assumption, to partially account for excitation modifications which result from plane-wave interaction with a side of an actual three-dimensional scatterer. The technique is based on incorporating the solution for a conducting wedge into the integral equations. Results are presented for coupling to coaxial connectors which are more consistent with experimental observations.

TABLE OF CONTENTS

INTRODUCTION 9

ANALYTIC EXPRESSIONS FOR THE RIGHT-ANGLE CONDUCTING WEDGE 14

APPLICATION TO THE COAXIAL-CONNECTOR COUPLING PROBLEM 15

EXPERIMENTAL COMPARISON 24

CONCLUDING REMARKS 26

ACKNOWLEDGMENTS 29

REFERENCES 30

LIST OF FIGURES

Figure		Page
1	Flush-mounted connector geometry for an infinite-ground-plane termination	11
2	Cross section of a connector situated on the aft of a weapon system	12
3	Analytical model used to calculate surface fields locally to a connector situated on a weapon system	13
4	Normalized normal electric field on the top surface of a right-angle conducting wedge with the aperture short-circuited. Fixed $k\rho_0$ values of the electric field as a function of incident angle are shown	16
5	Normalized normal electric field on the top surface of a right-angle conducting wedge with the aperture short-circuited. Fixed incident-angle values of the electric field as a function of $k\rho_0$ are shown	17
6	Normalized normal electric field on the top surface of a right-angle conducting wedge with the aperture short-circuited. Fixed incident-angle values of the electric field as a function of $k\rho_0$ are shown	18
7	Normalized surface current density on the top surface of a right-angle conducting wedge with the aperture short-circuited. Fixed $k\rho_0$ values of the surface current density as a function of incident angle are shown	19
8	Normalized surface current density on the top surface of a right-angle conducting wedge with the aperture short-circuited. Fixed incident-angle values of the surface current density as a function of $k\rho_0$ are shown	20
9	Normalized surface current density on the top surface of a right-angle conducting wedge with the aperture short-circuited. Fixed incident-angle values of the surface current density as a function of $k\rho_0$ are shown	21
10	Shifted coordinate system for merging the two models	23

11 Experimental set-up 25

12 Comparison of measurement and theory for the time-averaged received power with respect to 1 Watt. a=1.27 cm, b=3.02 cm, E_0=1 V/m. The incident wave was TE to x, and the axis of the connector was 25 cm from the x-directed edge 27

13 Further theoretical results for the configuration described in Figure 12. The effective area based on a line-matched termination is shown. The (line-matched) effective area was calculated from the received time-averaged power by forming $2\ \eta_0\ P/(E_0)^2$, where η_0 denotes the impedance of free space and P denotes the time-averaged power 28

INTRODUCTION

For linear and isotropic media, aperture penetration problems are often decomposed into three constituent electromagnetic components in the region external to the aperture. Specifically, a free-space incident field, a field component scattered by the obstacle with the aperture short circuited, and an external "perturbed-field component" due to the fields in the aperture itself. The fields in the interior region are coupled to the fields within the aperture through an appropriate Green's function. The first two components of the external problem are often considered to be "excitation terms." For problems in which the geometry is separable, these terms are generally straightforward to determine. The perturbed component, however, is often impossible to determine exactly even for separable geometries and simple aperture shapes. An integral equation statement for the aperture fields can usually be made in the general case; however, the interior and exterior Green's functions are often not known, and even in the special cases when they are known the solution of the integral equation will be difficult. Thus, to make the solution of aperture penetration problems tractable, simplifying assumptions are usually introduced.

For geometries which do not have many reflection boundaries, a common simplification is to make the purely mathematical assumption that the aperture is located on a flat conducting plane of infinite extent. The assumption is convenient mathematically because the external Green's function associated with the perturbed component is well known and of simple structure (at least for the case of a homogeneous exterior region). For sufficiently high frequencies this assumption is often physically reasonable (for the external problem) locally to the aperture. However, the infinite-ground-plane assumption is generally not appropriate for

calculating the aperture-short-circuited reflected-field component. Although this point should be obvious in many situations, the assumption is occasionally used in practice with unknown consequences. A subtle example which demonstrates some of the consequences is considered in this paper. The example was chosen because of its practical significance, and the fact that the example does not initially appear as though significant errors will be introduced by adopting the infinite-plane assumption when the reflected-field component is calculated.

The problem of interest is that of an exposed coaxial connector situated on a weapon system. The mathematical model for this problem has been exclusively based on a coaxial waveguide which terminates at a conducting plane (flange) of infinite extent [1]. For this configuration, the problem lends itself quite naturally to an integral-equation description for the aperture electric-field distribution which is solvable by the moment-method technique. For a TM (to z) incident plane wave, as shown in Figure 1, the effective height of the connector [1] is maximized when the incident wave is at the grazing angle $\theta_i=0$ for the case $k\rho<1$. This is because the quasi-static effective height of the connector is dependent on the total charge on the top surface of the central post, and this is maximized for $\theta_i=0$. Consequently, one is tempted to assume that the maximum quasi-static effective height for the connector on the actual weapon is obtained for the broadside incident wave as shown in Figure 2. However, experimental measurements have shown that the effective height (area) of aft-mounted multi-pin connectors is maximized for angles of incidence far off broadside [2]. Thus, the broadside edge of the weapon which is parallel to $\bar{E}^i$ significantly modifies the surface charge on the aft. A more appropriate model is to use the wedge shown in Figure 3.

In a strict sense, the aperture penetration problem has been totally

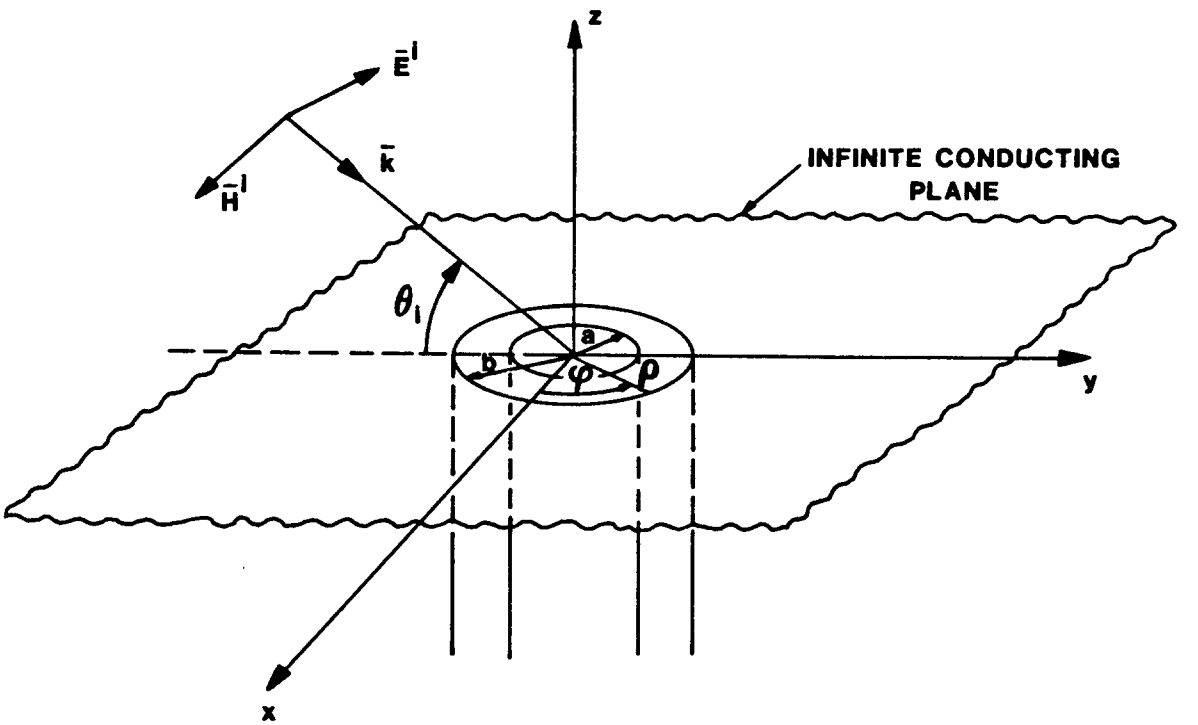

Figure 1: Flush-mounted connector geometry for an infinite-ground-plane termination.

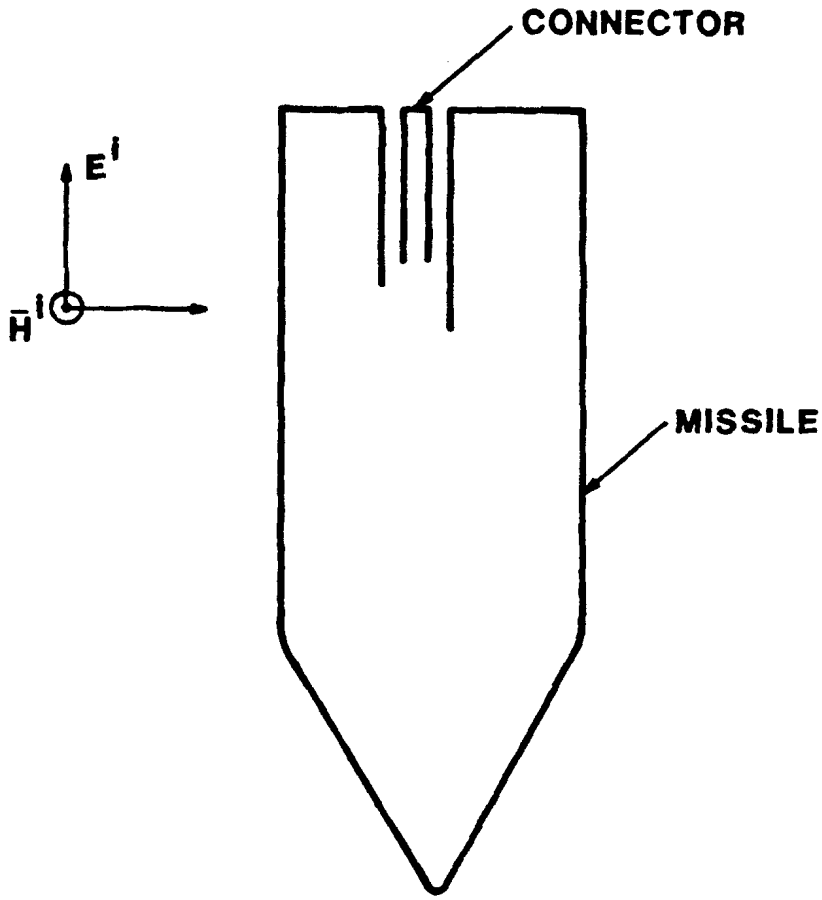

Figure 2: Cross section of a connector situated on the aft of a weapon system.

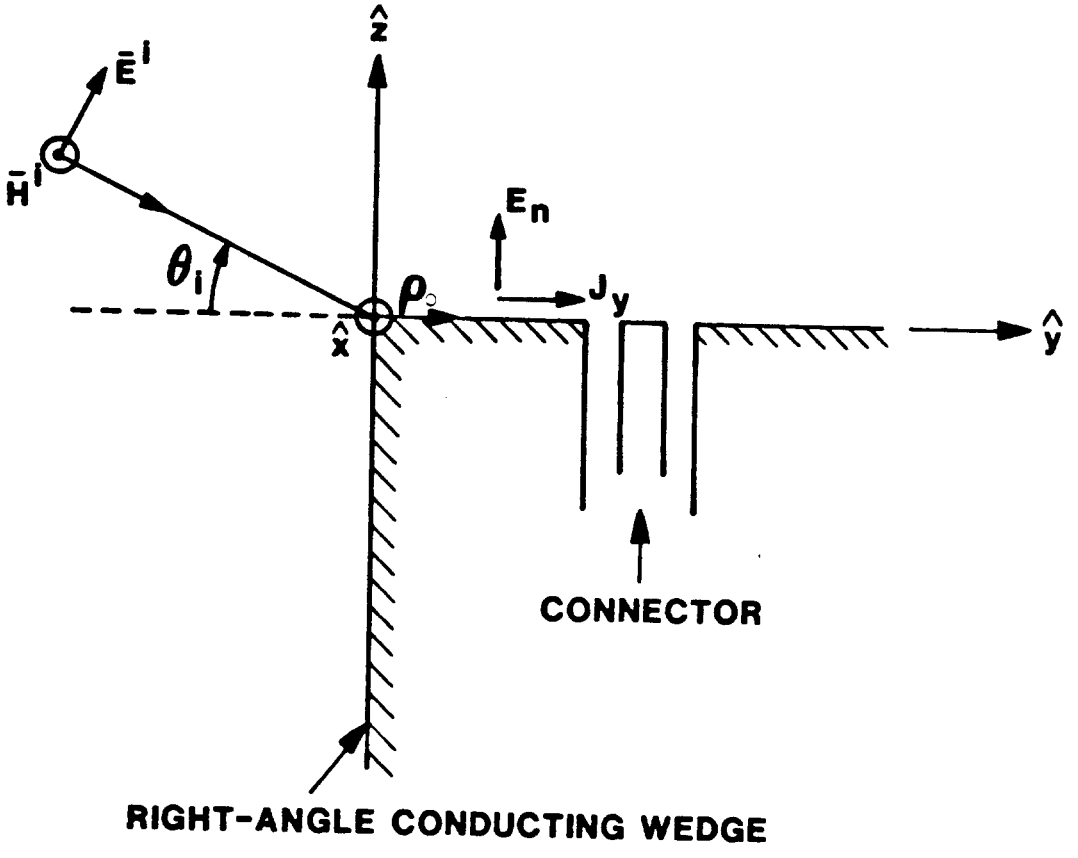

Figure 3: Analytical model used to calculate surface fields locally to a connector situated on a weapon system.

recast by placing the connector on the wedge. The Green's function for the wedge is considerably more complicated than for the infinite plane. Thus, specification of the external perturbed-field component due to the annular aperture is much more complicated as well. As noted, for sufficiently high frequencies the infinite-plane assumption is approximately valid locally to the aperture. In this case "sufficiently high" implies that the connector is a significant portion of a wavelength away from the edge. For frequencies that satisfy this constraint, a hybrid approach is suggested. Specifically, the wedge is used when calculating the excitation terms, whereas an infinite plane is used for the exterior perturbed component.

It is noted that similar hybrid formulations have been discussed in the literature. Notably, GTD/moment-method hybrid formulations have been successfully used for the problem of determining the plane-wave-induced surface current on monopole antennas which are situated on wedges or on finite ground planes [3]. This hybrid formulation, which modifies all three components of the coupling problem, is useful (and necessary) for geometries which involve many diffraction and/or reflection boundaries. For the class of interior coupling problems considered in this paper, it is shown that good results are obtainable by performing a straightforward modification of only the excitation terms. Though the success or failure of this approach is of course highly dependent on the geometry on which the aperture is located, there are many generic objects of interest to which this simpler approach can be successfully applied.

ANALYTIC EXPRESSIONS FOR THE RIGHT-ANGLE CONDUCTING WEDGE

For a TM or TE (to x) incident wave, the conducting-wedge problem is separable and the solutions are well known [4]. For the problem of

interest, only the TE (to x) case is required ($\bar{H}^i = \hat{x}\, H_o e^{jk\rho_o \cos(\pi-\theta_i)}$, where H_o denotes the peak amplitude). The surface normal electric field, E_n, is

$$\frac{E_n}{E_o} = -j\,\frac{4}{3}\,J_1(k\rho_o) + j\,\frac{8}{3}\sum_{n=1}^{\infty} e^{jn\pi/3}\,J'_{\frac{2n}{3}}(k\rho_o)\,\cos\left[\frac{2}{3}n(\pi-\theta_i)\right] , \tag{1}$$

where E_o denotes the peak electric-field amplitude of the incident wave. The surface current density, J_y, is given by

$$\frac{J_y}{H_o} = \frac{4}{3}\,J_o(k\rho_o) + \frac{8}{3}\sum_{n=1}^{\infty} e^{jn\pi/3}\,J_{\frac{2n}{3}}(k\rho_o)\,\cos\left[\frac{2}{3}n(\pi-\theta_i)\right] . \tag{2}$$

In these expressions, J_ν, where ν is a real number, denotes the standard Bessel function of the first kind, and k denotes the wavenumber. The derivative of J_ν with respect to its argument is denoted by J'_ν. An $\exp(j\omega t)$ time-convention was assumed. These functions are depicted in Figures 4 through 9 for various angles of incidence and values of $k\rho_o$. Several features associated with these figures are worth noting:

(1) Grazing incidence ($\theta_i = 0^o$) gives rise to a surface normal electric field (electrically removed from the edge) which is one-half the value obtained on an infinite ground plane; (2) At $\theta_i = 45^o$ the contribution due to the summation in Equation (1) vanishes in the limit $k\rho_o \to 0$, and therefore $|E_n|$ vanishes as $k\rho_o \to 0$; (3) For $\theta_i \neq 45^o$, $|E_n|$ exhibits the required cube-root edge singularity as $k\rho_o$ vanishes; (4) $|J_y/H_o| \to \frac{4}{3}$ as $k\rho_o \to 0$; (5) At $\theta_i = 0$, $|J_y/H_o| \to 1$ as $k\rho_o \to \infty$; (6) For $\theta_i \neq 0$, $|J_y/H_o| \to 2$ as $k\rho_o \to \infty$.

APPLICATION TO THE COAXIAL-CONNECTOR COUPLING PROBLEM

In reference [1], an integral equation was derived that describes the TM (to z) symmetric modes for the coaxial waveguide which terminates flush

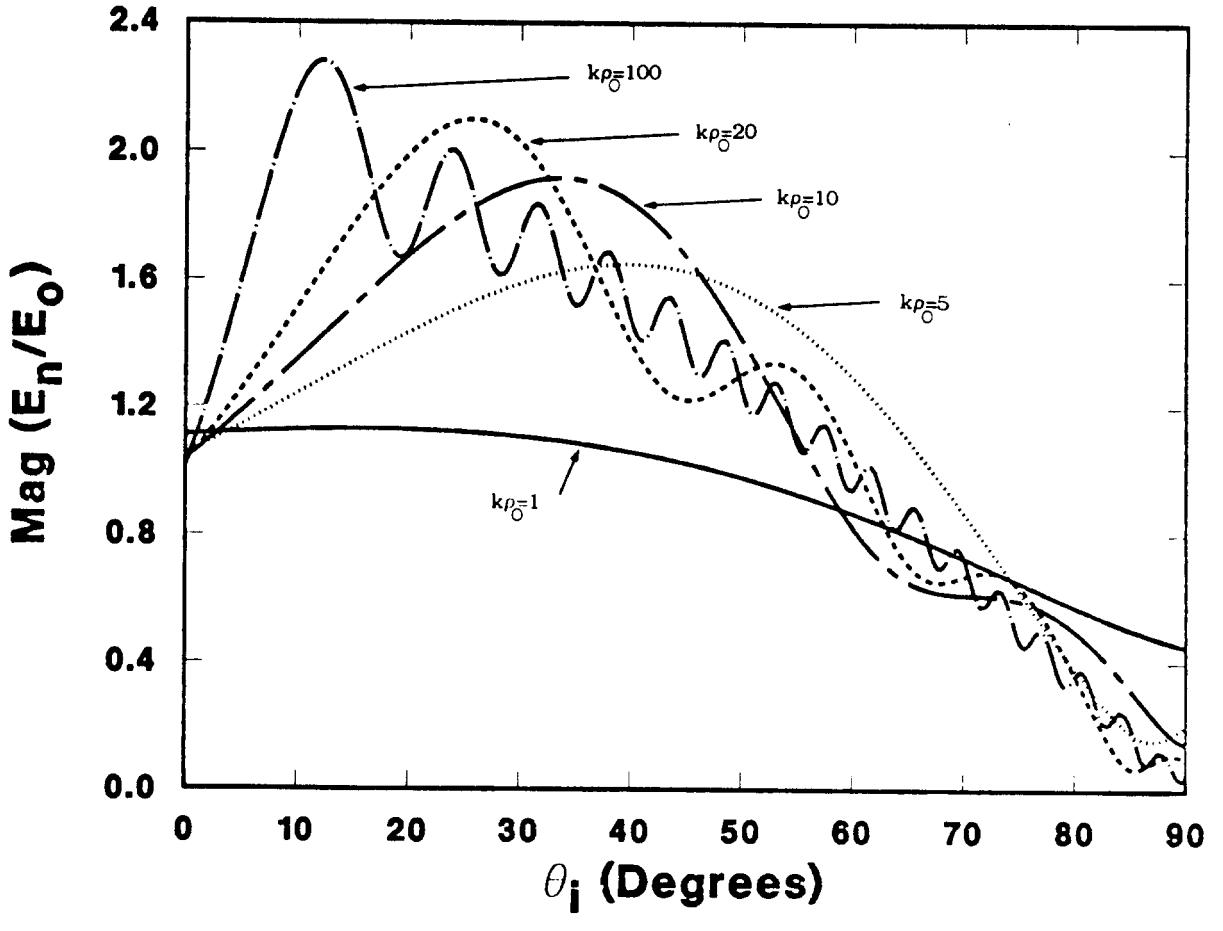

Figure 4: Normalized normal electric field on the top surface of a right-angle conducting wedge with the aperture short-circuited. Fixed $k\rho_o$ values of the electric field as a function of incident angle are shown.

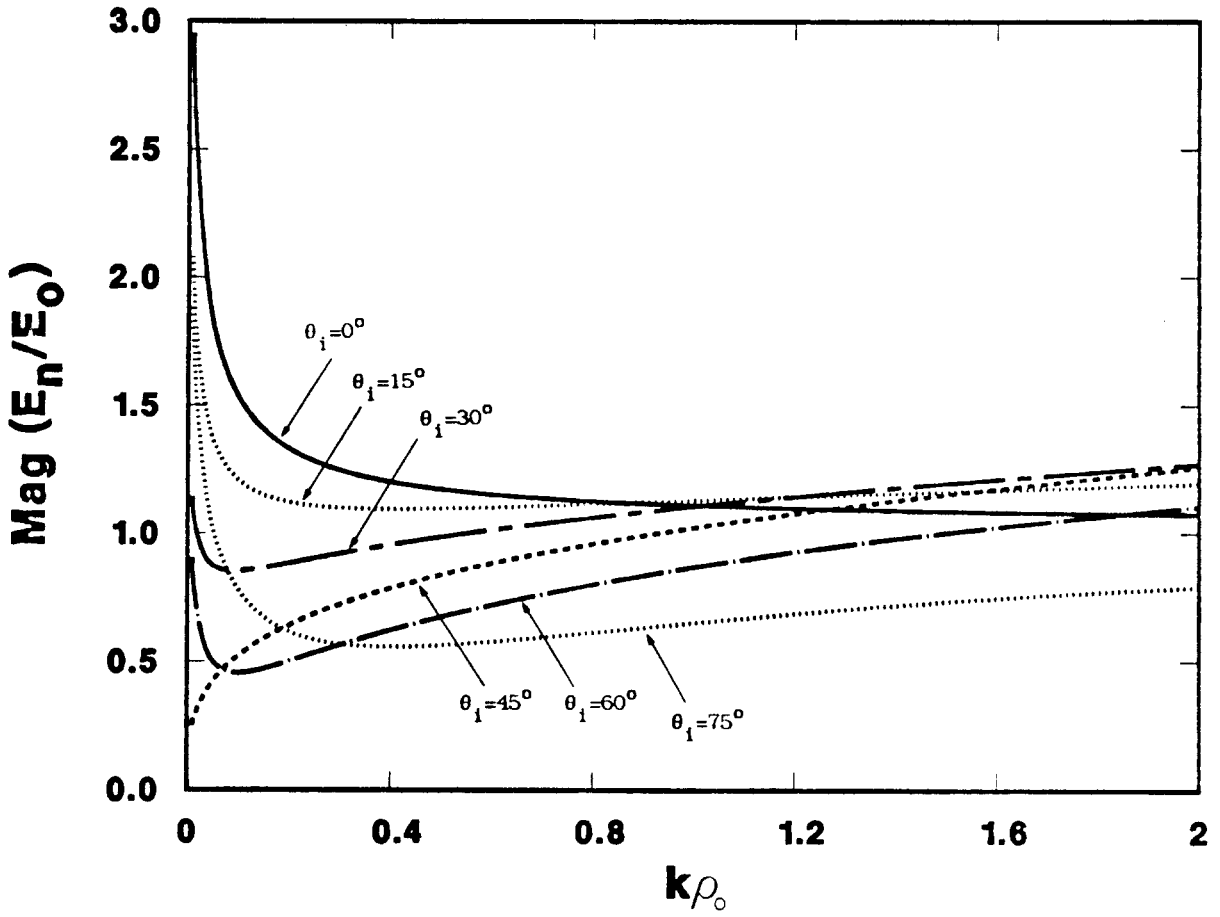

Figure 5: Normalized normal electric field on the top surface of a right-angle conducting wedge with the aperture short-circuited. Fixed incident-angle values of the electric field as a function of $k\rho_o$ are shown.

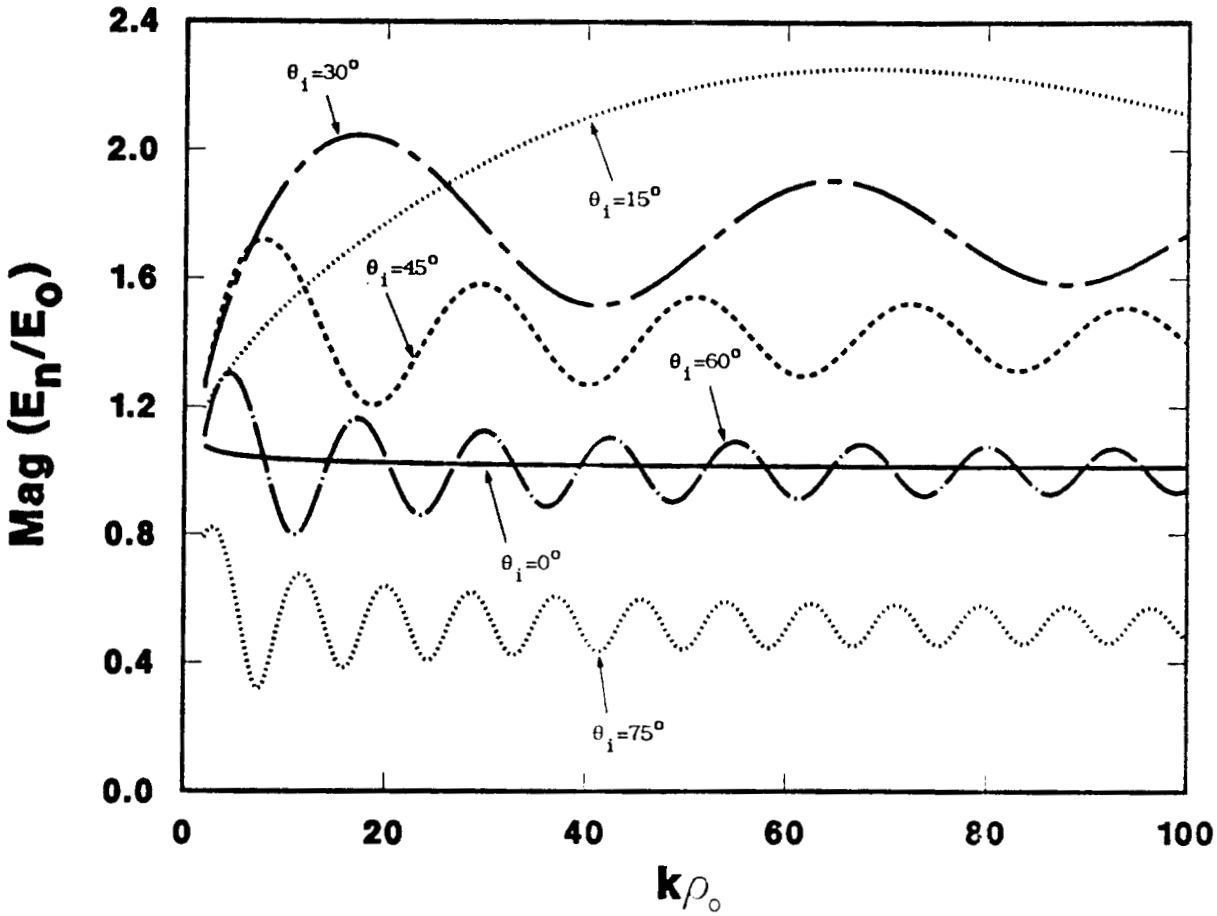

Figure 6: Normalized normal electric field on the top surface of a right-angle conducting wedge with the aperture short-circuited. Fixed incident-angle values of the electric field as a function of $k\rho_o$ are shown.

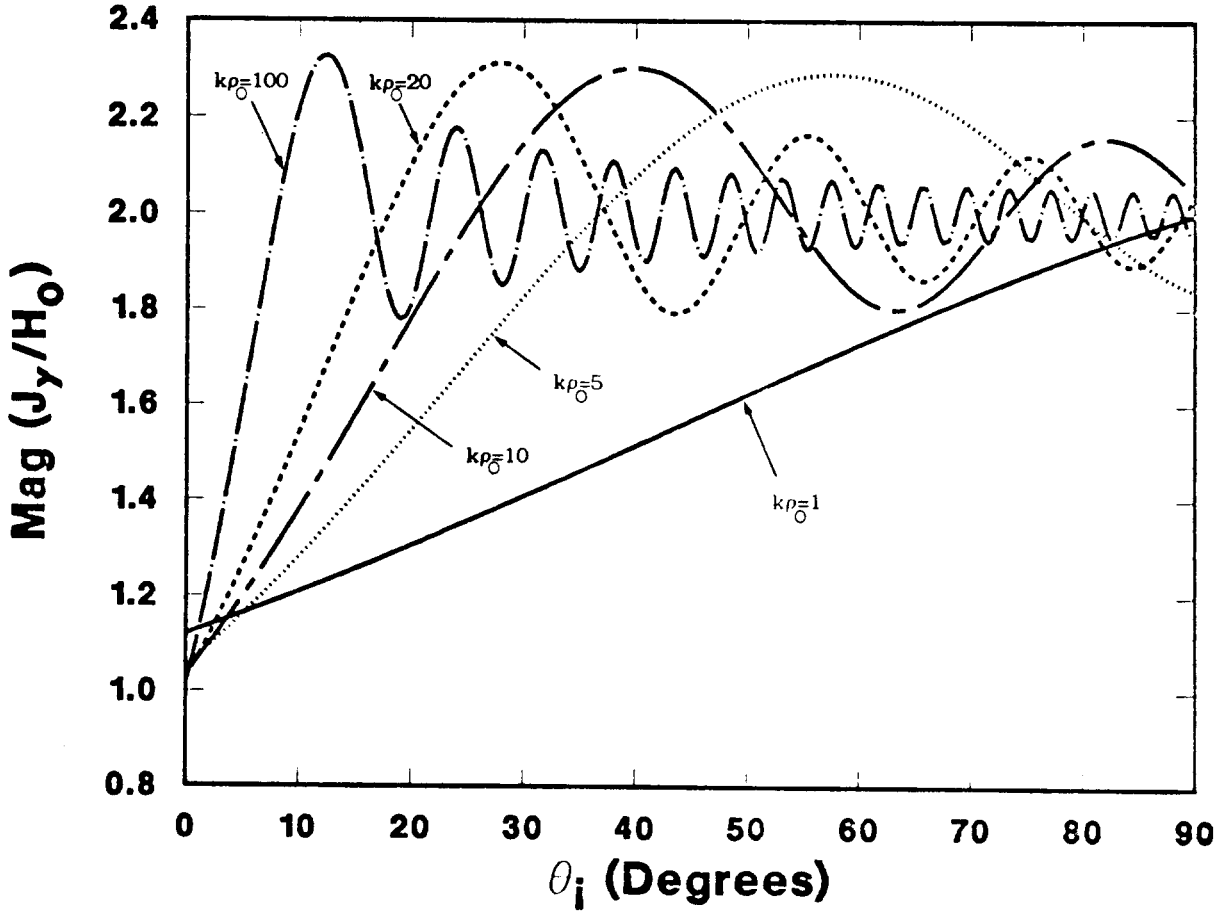

Figure 7: Normalized surface current density on the top surface of a right-angle conducting wedge with the aperture short-circuited. Fixed $k\rho_o$ values of the surface current density as a function of incident angle are shown.

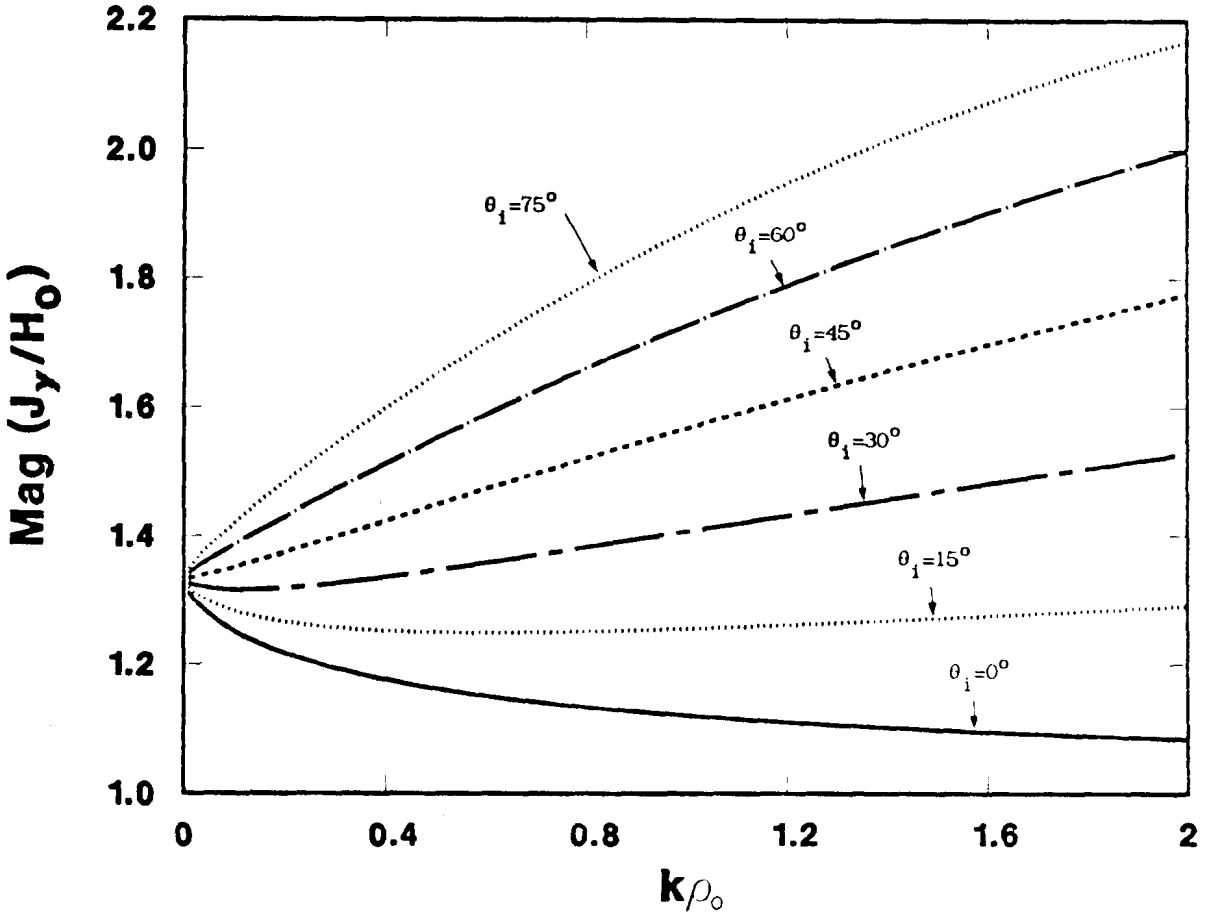

Figure 8: Normalized surface current density on the top surface of a right-angle conducting wedge with the aperture short-circuited. Fixed incident-angle values of the surface current density as a function of $k\rho_o$ are shown.

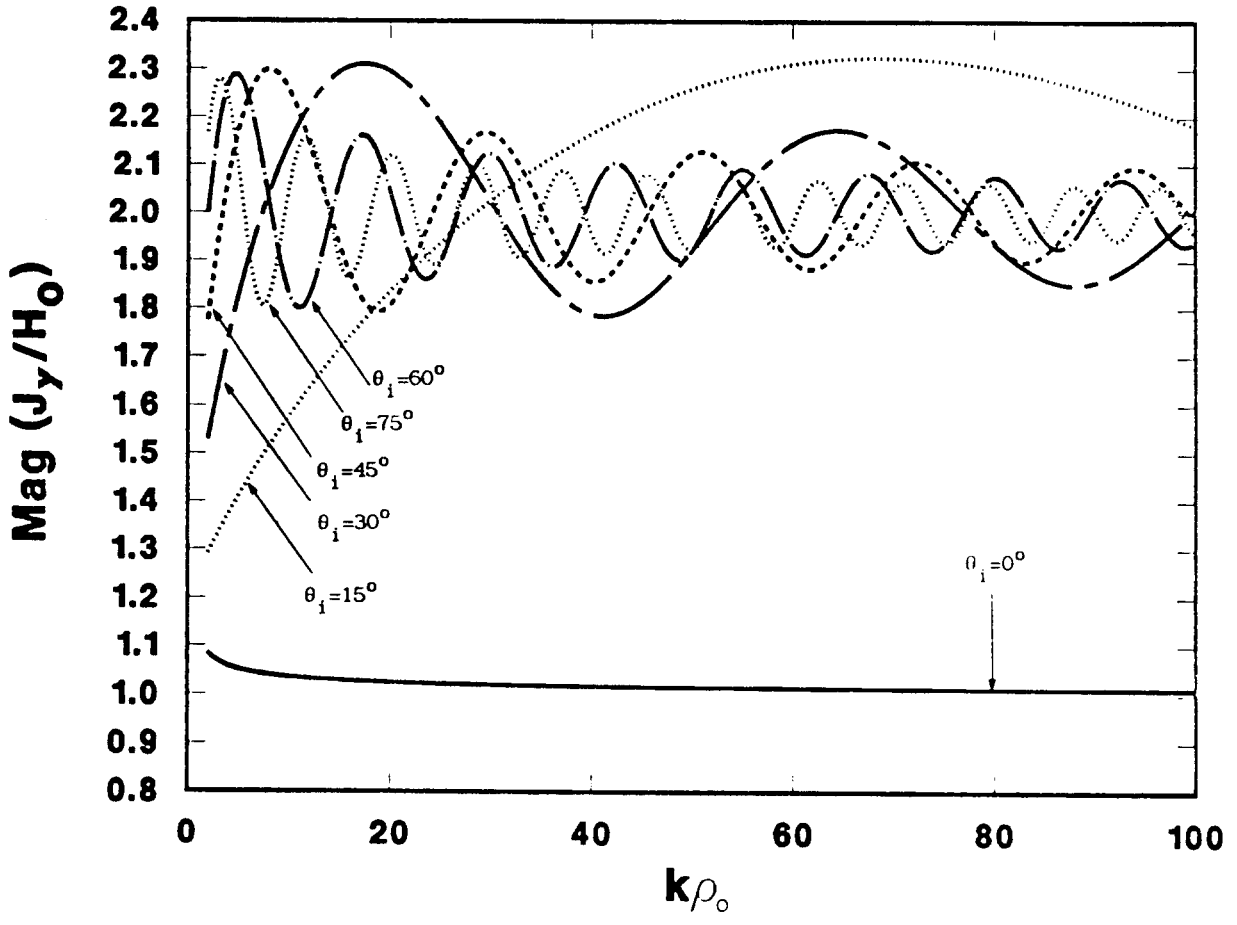

Figure 9: Normalized surface current density on the top surface of a right-angle conducting wedge with the aperture short-circuited. Fixed incident-angle values of the surface current density as a function of $k\rho_o$ are shown.

with a conducting plane of infinite extent. The basis for this equation was continuity of the azimuthal component of the magnetic field through the aperture. For TM (to z) plane-wave excitation (such that $\bar{H}^i = \hat{x}H_o e^{jk\rho\cos(\pi-\theta_i)}$) this integral equation is given by

$$\int_a^b d\rho' \; \rho' \; E_{\rho_o}(\rho') \; \mathcal{K}_{2_o}(\rho,\rho') = -j \; 2 \; H_o \; J_1(k\rho \; \cos(\pi - \theta_i)) \; , \; a<\rho<b, \qquad (3)$$

where the kernel, $\mathcal{K}_{2_o}$, is given in [1], and E_{ρ_o} denotes the unknown radial aperture electric field which gives rise to the TM (to z) symmetric modes in the coaxial waveguide. The term on the right side of (3) denotes the symmetric component of the TM (to z) free-space incident plane wave and the aperture-short-circuited reflected wave. This is the term which will be modified by the wedge solution. For this purpose, it is necessary to introduce a shifted coordinate system as shown in Figure 10. The axis of the coaxial waveguide is located a distance y from the edge of the wedge.

Because the integral equation is based on the azimuthal component of the magnetic field, it is necessary to write wedge solution (2) as $J_y\hat{y} = H_x\hat{x} = -\hat{\varphi} \; H_x\sin\varphi + \hat{\rho} \; H_x\cos\varphi$, and then use the term $-H_x\sin\varphi$. Finally, because the symmetric component of this term is required, it is necessary to average over φ. Therefore, to incorporate the effect of the wedge on the excitation term in integral equation (3), the right-hand side of (3) is replaced by

$$-\frac{4}{3} H_o \sum_{n=0}^{\infty} \epsilon_n \; e^{jn\pi/3} \; \cos\left[\frac{2}{3}n(\pi-\theta_i)\right] \left\{ \frac{1}{2\pi} \int_0^{2\pi} d\varphi \; \sin\varphi \; J_{\frac{2n}{3}}(ky + k\rho \; \sin\varphi) \right\} , \qquad (4)$$

where $\epsilon_n=1$ for n=0 and $\epsilon_n=2$ for $n\geq 1$, and ρ_o in (2) has been replaced by

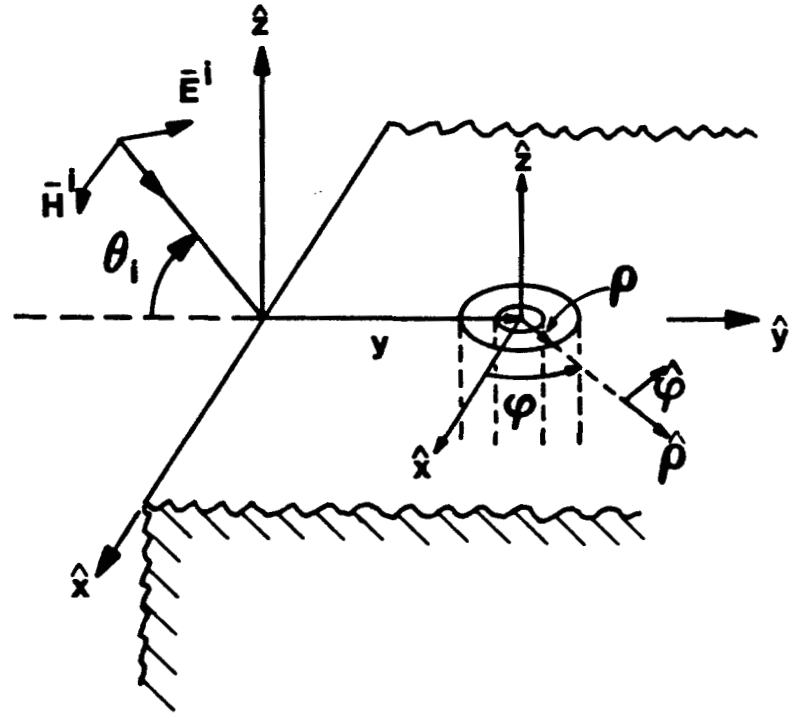

Figure 10: Shifted coordinate system for merging the two models.

$y+\rho\sin\varphi$. This modification is appropriate for $y > \lambda+b$, where λ is the wavelength, and for $\bar{H}^i$ parallel to the edge of the wedge. The integral can be evaluated as a summation over products of Bessel functions [5]; however, the numerical evaluation of the integral representation is simpler to implement and more efficient to evaluate.

EXPERIMENTAL COMPARISON

Previous experimental studies have examined the (matched-load) effective area of commercially available multi-wire connectors placed within a conducting box [2]. The single-wire connector considered here represents a simplification of these actual devices. Thus, specific amplitudes predicted by the hybrid theory for a similar edge offset to the connector are expected to differ with the previous measurements. Basic trends, however, should be similar.

Measurements on a single-wire connector in a conducting box would allow a more direct comparison of both angular trends and specific amplitudes predicted by the theory. Since hardware was available that would allow such a measurement, we conducted a brief experimental study.

The test geometry was a large coaxial aperture centered on the face of an rf-tight box that was 50 cm on a side. The coax had an outer diameter, 2b, of 6.03 cm, and an inner diameter, 2a, of 2.54 cm, for a characteristic impedance of approximately 52 Ohms. The coax was 42 cm long, with the final 10 cm being a conical transition section that terminated in a standard type-N connector.

Figure 11 depicts the measurement set-up. A Wiltron Automated Scalar Network Analyzer system performed the transmit-receive-data recording functions. This system consists of a Model 6647A programmable sweep

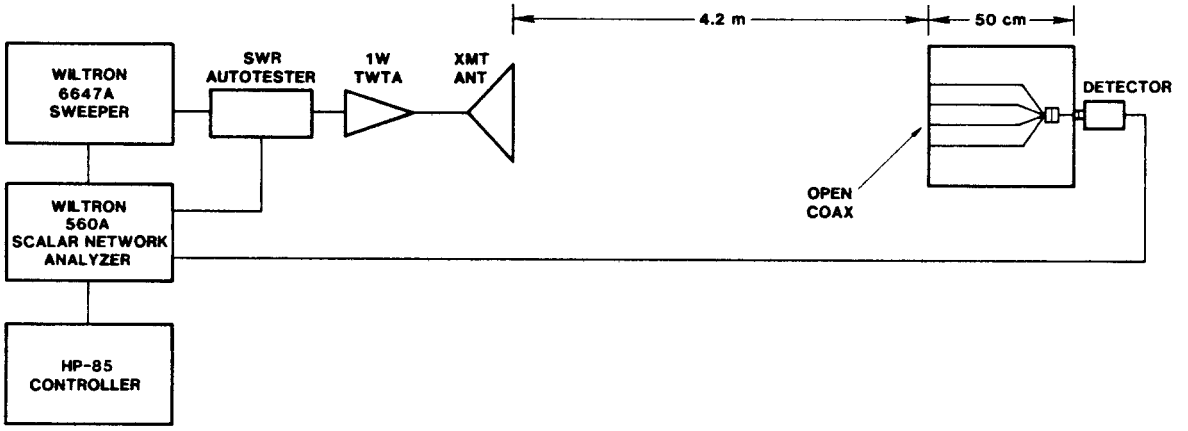

Figure 11: Experimental set-up.

generator, a Model 560A scalar network analyzer, a Model 85 controller, and controller software. To achieve the dynamic range we required, an external 1 W solid-state amplifier (1.7 to 4.2 GHz) was used.

We first characterized the incident field with a 2-5 GHz standard gain horn. We then measured the response of the open coax relative to the standard gain horn. These data, along with the calibration curve for the horn, allowed us to determine the power received by the open coax.

The results are shown in Figure 12 for the case of a termination which was matched to the line impedance. A moment-method numerical procedure was used for the solution of Eq. (3) with right-hand side given by (4). Note that the agreement in both the angular trend and the amplitude is quite good. Only a narrow bandwidth is displayed due to a suspected shunt-capacitance mismatch which became significant above 2.5 GHz at the transition from the large coax to the type-N connector. The accuracy of the hybrid model, however, should improve with increasing frequency (within the TM symmetric mode and moment-method limitations). The theoretical data is based only on TEM propagation; however, above 2.28 GHz the TE_{11} mode is above cutoff. The good agreement above this point clearly indicates the dominance of the TEM mode relative to TE_{11} when the incident wave excites both of these modes. As a final note, had the hybrid approach not been used to compute the theoretical results, the 30 degree and 0 degree curves would have essentially been reversed.

Additional theoretical results are shown in Figure 13.

CONCLUDING REMARKS

This paper was motivated by the fact that important angular dependence

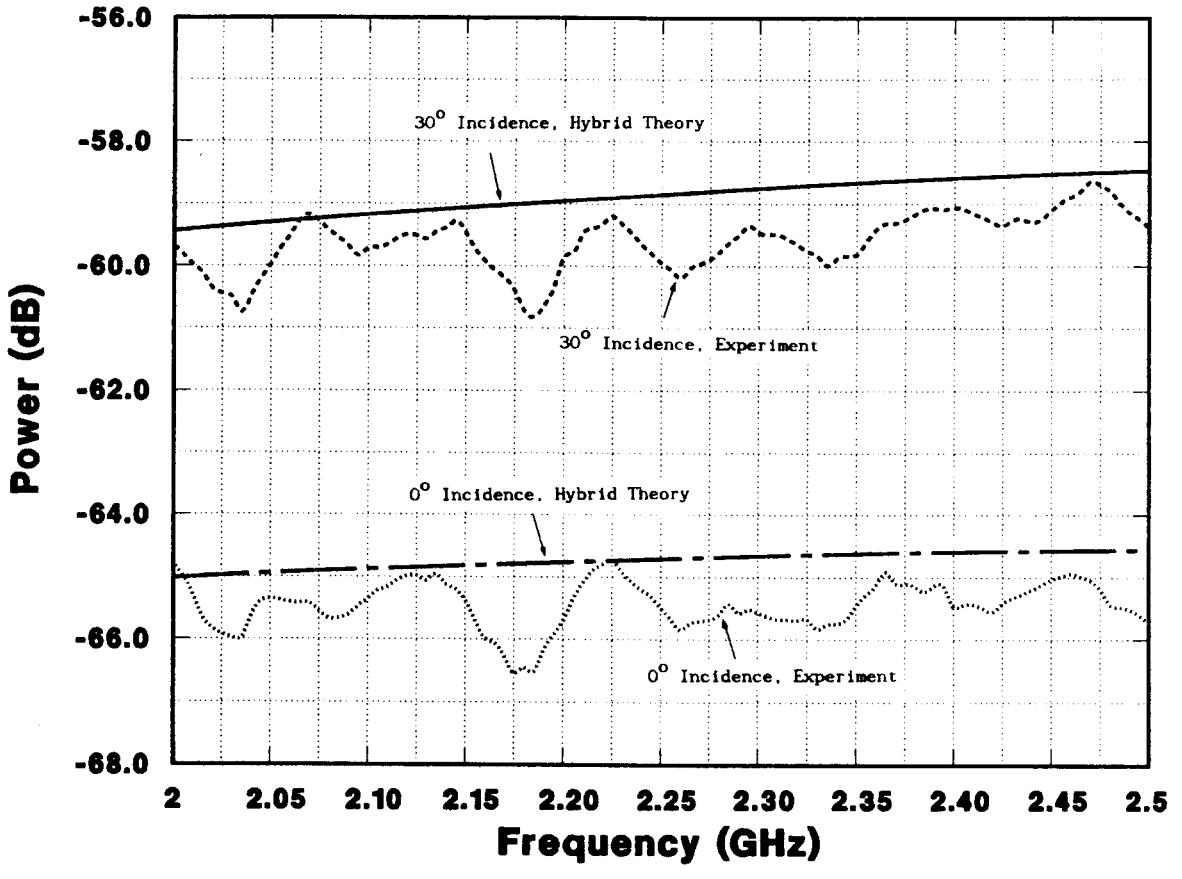

Figure 12: Comparison of measurement and theory for the time-averaged received power with respect to 1 Watt. a=1.27 cm, b=3.02 cm, E_o=1 V/m. The incident wave was TE to x, and the axis of the connector was 25 cm from the x-directed edge.

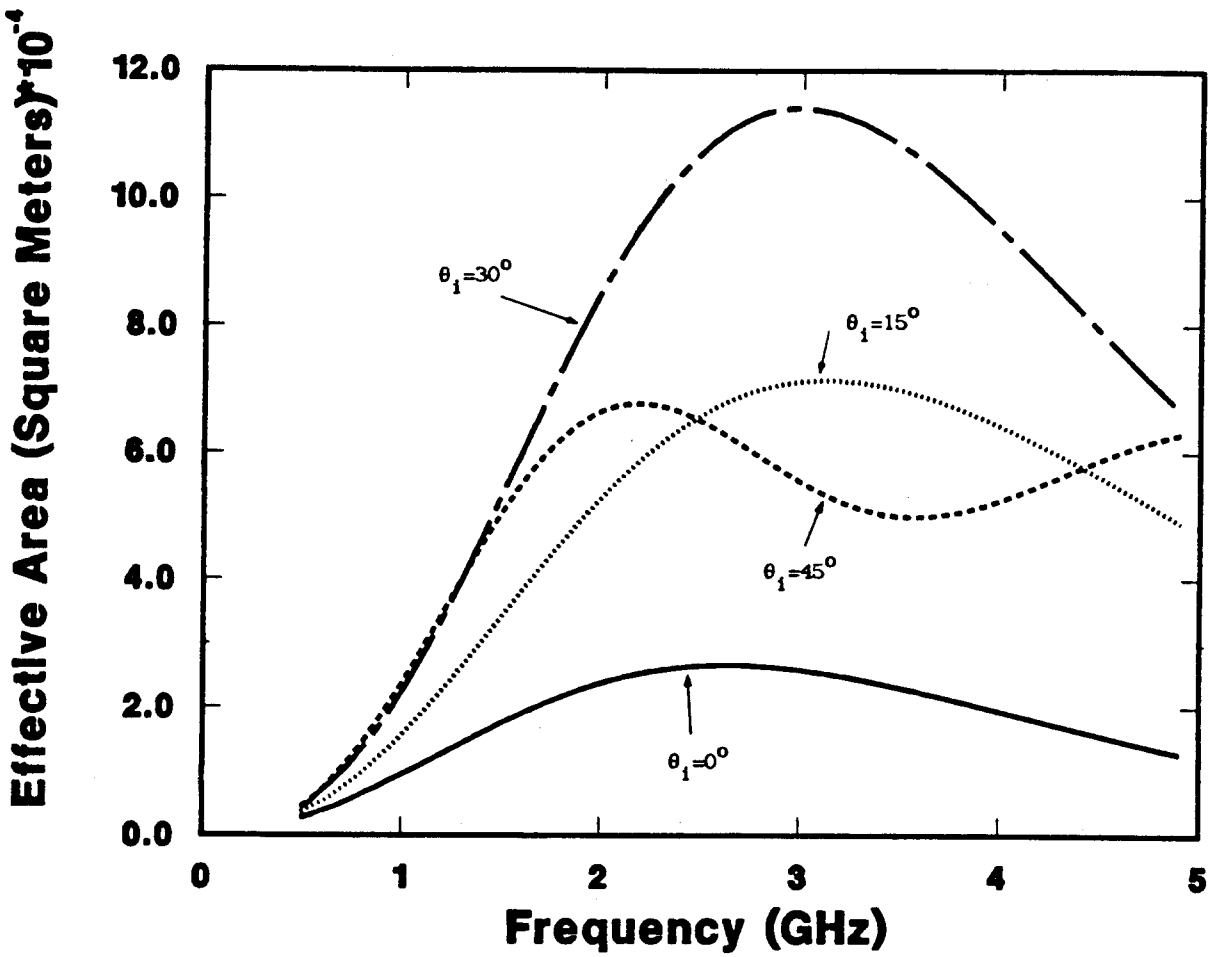

Figure 13: Further theoretical results for the configuration described in Figure 12. The effective area based on a line-matched load is shown. The (line-matched) effective area was calculated from the received time-averaged power by forming $2\ \eta_0\ P/(E_0)^2$, where η_0 denotes the impedance of free space and P denotes the time-averaged power.

associated with certain aperture-coupling problems is often inaccurately characterized by exclusively using an infinite-ground-plane assumption. The specific example considered was that of a connector on a weapon system. A simple theoretical technique was presented for modifying existing connector-coupling codes which are based exclusively on this assumption, to partially account for modifications in the excitation terms caused by the three-dimensional nature of actual weapons. Results obtained are much more consistent with experimental observations. Although the connector coupling example was the only one considered here, the technique should be useful for other similar types of aperture-coupling problems when corners are involved. Because only the excitation terms are modified, the limitation of the technique is that the aperture must not be electrically close to the edge of the wedge. More rigorous techniques could be adopted to accommodate this case [3].

For a given frequency and aperture offset from the edge of the wedge (ρ_o), one can obtain a quick approximation for the angle of incidence which will give rise to the greatest coupling by using the results for the surface fields for the conducting wedge presented in Figures 4 through 9.

For future study, it would be of interest to measure the power received by a single-wire connector placed at the end of a conducting cylinder, and compare those results with the rectangular-wedge hybrid theory.

ACKNOWLEDGMENTS

Appreciation is given to Richard P. Toth and John F. Aurand for their assistance in performing the experimental measurements.

REFERENCES

[1] Riley, D.J., *Analysis of the receiving characteristics of the circular diffraction antenna with both a flush-mounted and a recessed center post*, SAND-86-2398, Sandia Laboratories, November 1986.

[2] Bacon, L.D., "Coupling cross section to commericial flush-mounted female connectors," in *High-Power Microwave Research Quarterly Progress Report July-September 1985*, Ed. by J.M. Hoffman and J.E. Powell, SAND-86-0665, Sandia Laboratories, May 1986.

[3] Stutzman, W.L., and Thiele, G.A., *Antenna Theory and Design*, pp. 500-510, Wiley, New York, 1981.

[4] Harrington, R.F., *Time-Harmonic Electromagnetic Fields*, pp. 238-242, McGraw Hill, New York, 1961.

[5] Gradshteyn, I.S., and Ryzhik, I.M., *Table of Integrals, Series, and Products*, Fourth Edition, Academic, 1980

DISTRIBUTION:

Air Force Weapons Laboratory
Kirtland Air Force Base
Albuquerque, NM 87117
Attn: R. J. Hamilton, AFWL/TALR (1)
D. A. Knight, AFWL/TALV (1)
M. Skinner, AFWL/TALE (1)
T. Cetticeri, AFWL/TAL (1)
B. Anderson, AFWL/AWPB (1)
S. Bigelow, AFWL/AWPB (1)
W. Baker, AFWL/AWP (1)
D. Voss, AFWL/AWPB (1)
P. Vail, AFWL/TAL (1)
M. Hayworth (1)

Clemson University
Dept. of Electrical and Computer Engineering
Clemson University
Clemson, SC 29631
Attn: C. Butler (1)

Defense Nuclear Agency Headquarters
6801 Telegraph Rd.
Alexandria, VA 22310-3398
Attn: W. Goodell, Attn: SPLH (1)
P. Filios, Attn: RAEV (1)
G. Kwitkowski, Attn: RAEV (1)

EMA
1025 Hermosa S. E.
Albuquerque, NM 87108
Attn: D. E. Merewether (1)

General Dynamics-Pamona
401-01
P. O. Box 507
Pamona, CA 91769
Attn: R. McDonald (1)
K. Brown (1)

Harry Diamond Laboratory
2800 Powder Mill Rd.
Adelphi, MD 20783
Attn: L. F. Libelo (1)
A. Bromborsky (1)
J. Tatum (1)

JAYCOR
2100 Airpark Rd.
Suite 100 SE
Albuquerque, NM 87106
Attn: R. H. Bonn (1)

JAYCOR
11011 Torreyana Rd.
P. O. Box 85154
San Diego, CA 92121
Attn: E. P. Wenaas (1)
R. Leadon (1)

JAYCOR
39650 Liberty St.
Suite 320
Fremont, CA 94538
Attn: K. Casey (1)

Kaman Sciences
Dikewood Division
2800 28th St.
Suite 370
Santa Monica, CA 90405
Attn: K. Lee (1)
L. Marin (1)

Kaman Sciences
P. O. Box 7463
Colorado Springs, CO 80933
Attn: L. Allen (1)

Lawrence Livermore National Laboratory
University of California
P. O. Box 808
Livermore, CA 94550
Attn: S. C. Burkhart, L-387 (1)
R. J. King, L-156 (1)
H. G. Hudson, L-156 (1)
W. T. White, L-156 (1)
H. Cabayan, L-156 (1)
R. Mcleod, L-228 (1)
K. S. Yee, L-84 (1)

Los Alamos National Laboratory
University of California
P. O. Box 1663
Los Alamos, NM 87545
Attn: J. Toevs, MS-D408 (1)
J. Porter, MS-F617 (1)
B. Freeman, MS-J970 (1)
W. T. Armstrong, MS-D466 (1)
D. Bergan, MS-B218 (1)

Naval Research Laboratory
4555 Overlook Ave. SW
Washington, D. C. 20375-5000
Attn: A. W. Ali (1)
W. M. Manheimer (1)

Texas A&M University
Dept. of Electrical Engineering
College Station, TX 77843
Attn: R. D. Nevels (1)

U. S. Army Vulnerability Assessment Laboratory
White Sands Missile Range, NM 88002-5513
Attn: R. Flores (1)

Virginia Polytechnic Institute
Dept. of Electrical Engineering
Blacksburg, VA 24061
Attn: W. A. Davis (1)
W. L. Stutzman (1)

1000 V. Narayanamurti
1200 J. P. VanDevender
1230 J. E. Powell
1231 J. R. Lee
1232 W. Beezhold
1233 L. M. Choate
1234 R. J. Leeper
1235 J. M. Hoffman (6)
1235 J. F. Aurand
1235 L. D. Bacon (6)
1235 M. C. Clark
1235 L. D. Roose
1235 M. H. Ruebush
1235 R. P. Toth
1236 G. A. Zawadzkas
2000 L. K. Anderson
2300 J. L. Wirth
2320 J. H. Renken
2321 E. F. Hartman
2322 G. J. Scrivner
2322 C. D. Turner
2322 C. N. Vittitoe
2322 G. A. Seely
2322 J. D. Kotulski
2322 D. J. Riley (12)
3141 S. A. Landenberger (5)
3151 W. L. Garner (3)
3154-3 (28)
7550 T. S. Edrington
7553 M. E. Morris
7553 L. K. Warne
7554 L. D. Scott
7555 B. Boverie
7555 J. E. Solberg
7555 J. Gomez
8024 P. W. Dean